# Prdm16 is a physiologic regulator of hematopoietic stem cells

*Francesca Aguilo,[1] *Serine Avagyan,[1] Amy Labar,[1] Ana Sevilla,[1] Dung-Fang Lee,[1] Parameet Kumar,[1] Ihor R. Lemischka,[1] Betty Y. Zhou,[1] and Hans-Willem Snoeck[1]

[1]Department of Gene and Cell Medicine and Black Family Stem Cell Institute, Mount Sinai School of Medicine, New York, NY

**Fetal liver and adult bone marrow hematopoietic stem cells (HSCs) renew or differentiate into committed progenitors to generate all blood cells. *PRDM16* is involved in human leukemic translocations and is expressed highly in some karyotypically normal acute myeloblastic leukemias. As many genes involved in leukemogenic fusions play a role in normal hematopoiesis, we analyzed the role of *Prdm16* in the biology of HSCs using *Prdm16*-deficient mice. We show here that, within the hematopoietic system, *Prdm16* is expressed very selectively in the earliest stem and progenitor compartments, and, consistent with this expression pattern, is critical for the establishment and maintenance of the HSC pool during development and after transplantation. *Prdm16* deletion enhances apoptosis and cycling of HSCs. Expression analysis revealed that *Prdm16* regulates a remarkable number of genes that, based on knockout models, both enhance and suppress HSC function, and affect quiescence, cell cycling, renewal, differentiation, and apoptosis to various extents. These data suggest that *Prdm16* may be a critical node in a network that contains negative and positive feedback loops and integrates HSC renewal, quiescence, apoptosis, and differentiation. (*Blood*. 2011;117(19):5057-5066)**

## Introduction

Hematopoietic stem cells (HSCs) can self-renew and differentiate into all cell types of the hematopoietic system and are regulated by interacting intrinsic and extrinsic mechanisms.[1] Among intrinsic mechanisms, several transcriptional regulators involved as partners of leukemogenic fusion proteins, such as *Mll*[2-4] and *Evi1*,[5] are required for normal HSC function, whereas others, such as *Runx1*[6,7] and *Scl*,[8,9] are essential for the establishment of HSCs during development. PR domain-containing 16 (*PRDM16*), a 140-kDa zinc finger protein, was originally discovered as a fusion partner in t(1:3)(p36;q21) translocations in acute myeloblastic leukemia (AML)[10,11] and later in t(1;21)(p36;q22) translocations fused to *RUNX1*.[12,13] In addition, elevated *PRDM16* expression, because of promoter hypomethylation, is frequently observed in karyotypically normal AML.[14] Deletion of the PR domain, which shows homology with a SET chromatin remodeling domain and is also present in *EVI1*,[10] appears important for the leukemogenic properties of human *PRDM16*. Translocations involving *PRDM16* invariably delete the PR domain,[10-13] whereas PR-deleted *Prdm16* causes AML in $p53^{-/-}$ mice.[14] Furthermore, both *Prdm16* and *Evi1* are frequent targets of insertional mutagenesis in mice, causing deletion of the PR domain.[15] Overexpression of *Prdm16* expands HSCs in vitro. However, these expanded HSCs cause a myeloproliferative disease after transplantation.[16] *Prdm16* has also been shown to be critical for the development of brown adipose tissue in the mouse. PRDM16 is a transcriptional cofactor and interacts with the ligand-activated transcription factor peroxisome proliferator-activated receptor-γ and with CCAAT/enhancer-binding protein-β.[17,18]

Although its involvement in leukemic translocations and high expression in karyotypically normal AML suggest a physiologic role for *Prdm16* in hematopoiesis, this role has not been established yet. Therefore, we analyzed the role of *Prdm16* in hematopoiesis.

## Methods

### Mice

C57BL/6J mice (CD45.2$^+$ B6) were purchased from The Jackson Laboratory and C57BL/6.SJL-*Ptprca*$^{Pep3b/BoyJ}$ (CD45.1$^+$ B6 mice) from the National Cancer Institute. Sperm from *Prdm16*$^{Gt(OST67423)Lex}$ mice (Lexicon Genetics)[19] was reconstituted by in vitro fertilization in the Mouse Genetics Shared Resource of the Mount Sinai School of Medicine. Animals were housed in a specific pathogen-free facility. Experiments and animal care were performed in accordance with the Mount Sinai Institutional Animal Care and Use Committee.

### Mouse genotyping

Genotyping for *Prdm16* was done using a forward primer in gene-trap vector (5′-AAATGGCGTTACTTAAGCTAGCTTGC-3′) and in intron 1 (5′-AAATGGCGTTACTTAAGCTAGCTTGC-3′) and a reverse primer in exon 2 (5′-CCATCTGAGGTCGTCTGAAACTGG-3′), yielding a 231-bp band from a wt allele and a 122-bp band from a deleted allele.

### Antibodies and cytokines

Fluorescein isothiocyanate-conjugated anti-CD2, anti-CD3ε, anti-CD8α, anti-CD4, anti-CD19, anti-B220, anti-Gr1, anti-Mac1, anti-CD48, phycoerythrin-conjugated anti-Flt3, PECy7-conjugated streptavidin, and allophycocyanin-AlexaFluor-750-conjugated anti-c-kit were purchased from eBioscience. Fluorescein isothiocyanate-conjugated anti-CD41, phycoerythrin-conjugated anti-Sca1, anti-CD34, peridinin chlorophyll protein-Cy5.5-conjugated anti-Mac1, streptavidin, allophycocyanin-conjugated anti-c-kit, anti-IgM, goat

Submitted July 31, 2010; accepted January 17, 2011. Prepublished online as *Blood* First Edition paper, February 22, 2011; DOI 10.1182/blood-2010-08-300145.

*F.A. and S.A. contributed equally to this study.

The publication costs of this article were defrayed in part by page charge payment. Therefore, and solely to indicate this fact, this article is hereby marked "advertisement" in accordance with 18 USC section 1734.

anti-rat antibody, PerCP-conjugated streptavidin, PECy7-conjugated anti-CD19, anti-hCD4, allophycocyanin-Cy7–conjugated streptavidin, anti-CD19, anti-CD8, and Pacific blue-conjugated anti-B220 were purchased from BD Biosciences PharMingen. Phycoerythrin-, allophycocyanin-, and PECy7-conjugated anti-CD150 and Pacific blue-conjugated anti-Sca1 were purchased from BioLegend. Lineage cocktail included CD2, CD3ϵ, CD8α, CD4, CD19, B220, Gr1, Mac1, and Ter119, as well as CD41 and CD48 when noted,

### Cell sorting and flow cytometry

Bone marrow (BM) and fetal liver (FL) cells were isolated by cell sorting as described previously.[20] Flow cytometric analysis was performed on a 5-laser LSRII with DiVa software (BD Biosciences) and analyzed using FlowJo software. For analysis of β-galactosidase activity in *Prdm16*$^{+/-}$ BM cells, $5 \times 10^6$ *Prdm16*$^{+/-}$ or wt BM cells were resuspended in 100 μL of phosphate-buffered saline/2% fetal calf serum before loading with 100 μL of 2mM fluorescein di-D-β-galactopyranoside (Invitrogen) in $dH_2O$ and followed by incubation at 37°C for 60 seconds. Uptake was stopped by addition of 10 volumes of ice-cold phosphate-buffered saline/2% fetal calf serum, and the reaction was allowed to proceed for 1 to 3 hours on ice in the dark. 4,6-diamidino-2-phenylindole (1 μg/mL, Sigma-Aldrich) was added before analysis, for dead cell exclusion. For measurement of apoptosis, FL cells were stained with the HSC cocktail, washed and resuspended at $0.5 \times 10^6$ cells/200 μL in binding buffer, and stained with annexin V-phycoerythrin (BD Biosciences, PharMingen) as recommended by the manufacturer.

### Colony assays

A total of $2.5 \times 10^4$ E15 to E18 FL cells/mL were plated in triplicate in 35-mm nontissue culture plates in methylcellulose M3434 medium supplemented with recombinant cytokines according to the manufacturer's instructions (StemCell Technologies). Myeloid and erythroid colony formation was scored after 7 days.

### Quantitative RT-PCR

Total RNA, isolated using RNeasy Mini Kit (QIAGEN), was reverse-transcribed with SuperScript III (Invitrogen), according to the manufacturer's instructions, and cDNA was amplified with a specific primer and probe mix for *Prdm16* (TaqMan Gene Expression Assay, Applied Biosystems), using 18S RNA as an internal control. Thermal cycling conditions were 95°C for 10 minutes, 40 cycles of 95°C for 15 seconds, and 60°C for 1 minute on a StepOnePlus Real-Time PCR System. Analysis was done using the comparative threshold cycle ($C_t$) method ($\Delta\Delta C_t$).

### Gene expression analysis

Five LSKCD150$^+$ FL cells from E15 *Prdm16*$^{-/-}$ and wt littermate mice were sorted directly into the mixture of CellsDirect 2x Reaction Mix (CellsDirect One-Step qRT PCR Kit, Invitrogen), 0.2x TaqMan Assay Mix (Applied Biosystems), and SuperScript III RT/Platinum Taq Mix (Invitrogen). Reverse transcription and specific target amplification were serially performed as follows: 15 minutes at 50°C, 2 minutes at 95°C, 22 cycles of 15 seconds at 95°C, and 4 minutes at 60°C. Preamplified cDNA was diluted with TE buffer (1:5) and was used for the real-time polymerase chain reaction (PCR). Gene expression was analyzed using BioMark 96–96 Dynamic Array (Fluidigm) using inventoried TaqMan Gene Expression Assay (Applied Biosystems). The PCR profile was 95°C for 10 minutes, followed by 40 cycles of 95°C for 15 seconds and 60°C for 1 minute. Data were analyzed using BioMark Real-Time PCR Analysis Software, Version 2.0 (Fluidigm), and the geometric mean of the $\Delta\Delta C_t$ values for the different sorted samples was represented.

### Transplantation assays

A total of 0.5 to $2 \times 10^6$ FL or BM cells (CD45.2$^+$, B6.129 background, the donor) were mixed with an equal number of T cell-depleted wt C57BL/6.SJL-*Ptprca*$^{Pep3b/BoyJ}$ (CD45.1$^+$B6) or CD45.1$^+$CD45.2$^+$ C57BL/6.SJL-*Ptprca*$^{Pep3b/BoyJ}$.C57BL/6F1 (CD45.1$^+$CD45.2$^+$B6) competitor BM cells, and injected into lethally irradiated (500 cGy followed by 700 cGy 3 hours later) B6.129F1 hosts (CD45.2$^+$). Wt controls were always littermates. After 12 to 16 weeks, peripheral blood (PB) and BM were analyzed. A total of $2 \times 10^6$ BM cells were then transplanted into lethally irradiated secondary B6.129F1 hosts. In transplantation experiments with purified cells, 300 BM LT-HSC (LSKCD150$^+$) or 500 LSK FL or adult BM LSK cells were mixed with 0.2 to $0.5 \times 10^6$ T cell-depleted wt CD45.1$^+$B6 or CD45.1$^+$CD45.2$^+$B6 BM cells. Reconstitution ratios were calculated by dividing the fraction of donor (CD45.2$^+$) to competitor (CD45.1$^+$ or CD45.1$^+$CD45.2$^+$) cells within the B (CD19$^+$) and myeloid (Mac1$^+$Gr1$^+$) lineages. Reconstitution ratios are a direct representation of the relative potency of the tested HSC populations. T cells were not analyzed, as donor and recipient could not be distinguished, and as remaining host-derived hematopoietic cells are mostly T cells after lethal irradiation.[20] To measure the effect of secondary transplantation, the logarithm of the reconstitution ratio was compared in primary and secondary hosts. An advantage of log transformation is that a ratio less than 1 will give a negative value, and negative ratios will extend over the same numerical range as positive ones (eg, a ratio of 0.01 gives a log ratio of −2, a ratio of 100 gives a log ratio of +2), thus normalizing the data.[21] Accordingly, data are presented as the difference between input log donor/competitor (ie, the log ratio in the primary recipient) and the output log donor/competitor (ie, the log ratio 3 months after reconstitution of the secondary recipients) and are referred to as Δ(log ratio).

### Homing assay

E18 FL cells were labeled with carboxyfluorescein diacetate succinimidyl diester (CFSE) according to manufacturer's instructions (Invitrogen). More than 99% of cells were stained, and fluorescence intensity ranged between $10^4$ and $10^5$. CFSE-stained cells from *Prdm16*$^{-/-}$, *Prdm16*$^{+/-}$, or wt mice were intravenously injected into B6.129F1 lethally irradiated mice (12 Gy, one dose). After 3 hours, the BM was harvested and homing efficiency was calculated as previously described.[22]

### Statistical analysis

For statistical analysis, paired or unpaired Student *t* test were used. When more than 2 groups were compared, one-way ANOVA was used. Results are expressed as mean ± SEM. Bonferroni correction was applied to determine statistically significant differences in Fluidigm expression analysis.

## Results

### Selective expression of *Prdm16* in the earliest stem and progenitor cells

We examined the expression pattern of *Prdm16* in the BM of *Prdm16*-deficient mice generated in a gene-trap screen using a LacZ-expressing vector. In these mice, *LacZ* insertion into the first intron of *Prdm16* leads to β-galactosidase expression under the control of endogenous *Prdm16* regulatory elements but termination of PRDM16 translation after the first exon (Figure 1A).[19] Flow cytometric LacZ staining using fluorescein di-D-β-galactopyranoside in adult heterozygous mice revealed exclusive expression in lineage$^-$Sca1$^+$kit$^+$ (LSK) hematopoietic stem and progenitor cells (HSPCs). Within the LSK population, expression was highest in short-term (ST, LSKCD34$^+$Flt3$^-$)[23] and long-term (LT, LSKCD34$^-$Flt3$^-$)[23] HSCs, and was lower in multipotential progenitors (MPPs, LSKCD34$^+$Flt3$^+$).[23] No LacZ was detected in common lymphoid progenitors (CLPs, lin$^-$Sca1$^{lo}$kit$^-$IL7Rα$^+$Flt3$^+$)[23] and lin$^-$Sca1$^-$kit$^+$ (LS$^-$K)[23] cells, which contain common myeloid, granulocyte/macrophage, and megakaryocyte/erythroid progenitors (Figure 1B). Similarly, quantitative PCR showed predominant expression of *Prdm16* mRNA in HSCs, although some

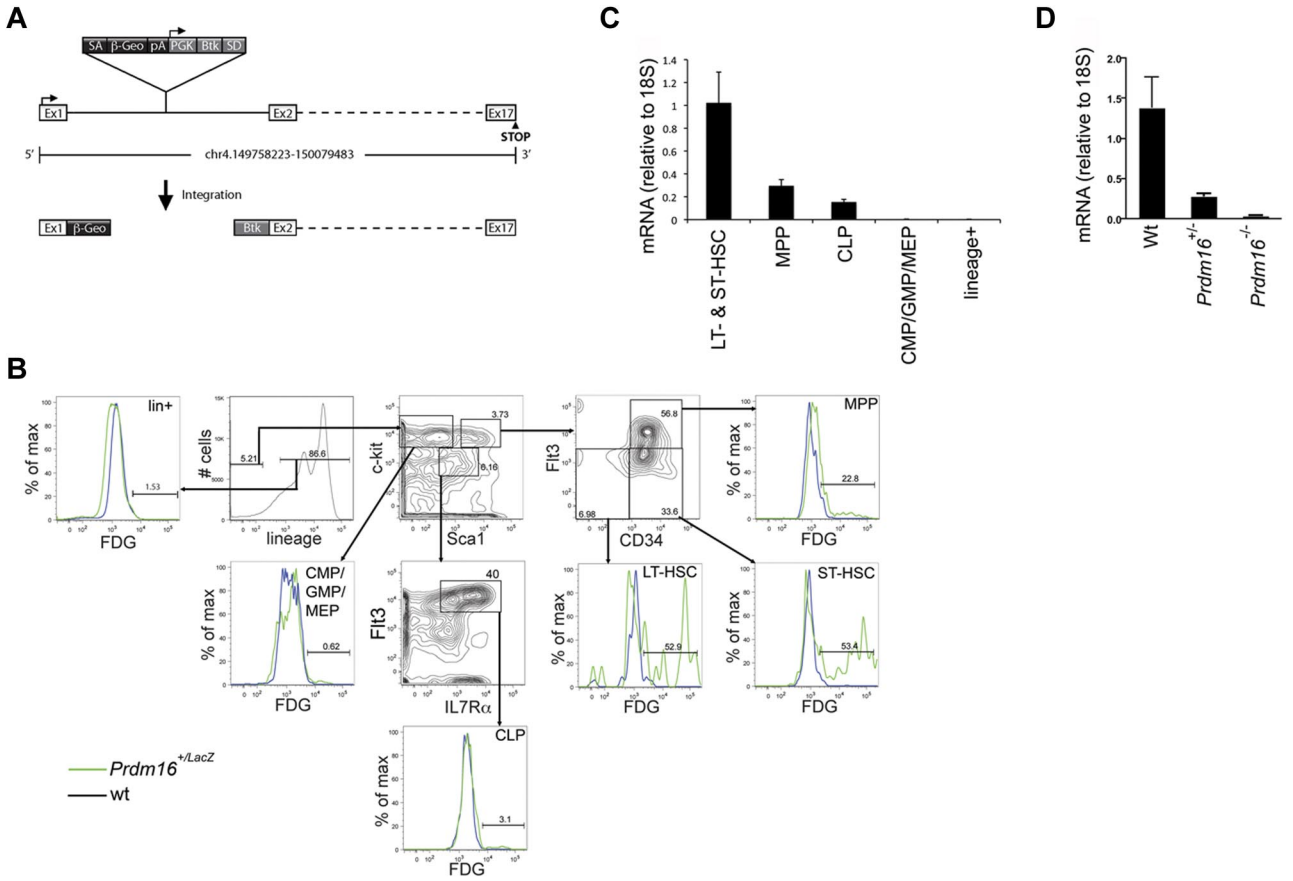


**Figure 1. Expression of *Prdm16* in adult BM.** (A) Schematic representation of the genomic *Prdm16* region in *Prdm16*$^{Gt(OST67423)Lex}$ (*Prdm16*$^{-/-}$) mice. Adapted from Zambrowicz et al[19] with permission. (B) Expression of LacZ, measured by flow cytometry after staining with fluorescein di-D-β-galactopyranoside, in the BM of *Prdm16*$^{Gt(OST67423)Lex/+}$ mice. CMP indicates common myeloid progenitor; GMP, granulocyte/macrophage progenitor; MEP, megakaryocyte erythroid progenitor; LT-HSC, long-term hematopoietic stem cell; and ST-HSC, short-term hematopoietic stem cell. (C) Expression of *Prdm16* mRNA in HSCs (LSKFlt3$^-$, composed of ST- and LT-HSCs), MPPs, CLPs, and lineage$^+$ cells (n = 3). (D) Expression of *Prdm16* mRNA in brain from *Prdm16*$^{-/-}$, *Prdm16*$^{+/-}$, and wt embryos.

expression of *Prdm16* mRNA was also observed in CLPs (Figure 1C). Next, we verified that *Prdm16* mRNA was undetectable in *Prdm16*$^{-/-}$ embryos. Although *Prdm16* mRNA was nearly undetectable in brains of *Prdm16*$^{-/-}$ embryos, expression was reduced to 20.2% ± 0.06% of that in wt controls in *Prdm16*$^{+/-}$ embryos, significantly different from the expected 50% ($P = .02$, Figure 1D) and indicating that *Prdm16* expression is haploinsufficient.

We conclude that *Prdm16* mRNA is expressed specifically in the most immature HSPCs and that *Prdm16*$^{+/-}$ mice are haploinsufficient with respect to *Prdm16* mRNA expression.

### Hematopoietic profile of *Prdm16*–deficient mice

When *Prdm16*$^{+/-}$ mice were mated, the distribution of genotypes among embryos at all stages of development followed Mendelian ratios (wt: 22; *Prdm16*$^{+/-}$: 47; *Prdm16*$^{-/-}$: 22). However, no *Prdm16*$^{-/-}$ live-born pups were ever observed, indicating that *Prdm16*$^{-/-}$ mice die during or very shortly after birth. Cellularity of FL and thymus of *Prdm16*$^{-/-}$ and *Prdm16*$^{+/-}$ embryos at E16 to E18 was similar to that of wt embryos (Figure 2A). In adult mice, cellularity of BM, spleen, and thymus was also similar in wt and *Prdm16*$^{+/-}$ mice (Figure 2A). However, total PB white blood cell counts in adult *Prdm16*$^{+/-}$ mice were higher than in wt mice (Figure 2B). As the distribution of B, T, and myeloid cells was similar, this increase involved all these lineages (Figure 2B). The fraction of developing B cells (AA4.1$^+$B220$^+$CD19$^-$ pre-pro-B cells, AA4.1$^+$B220$^+$CD19$^+$ pre- and pro-B cells, AA4.1$^+$IgM$^+$ immature B cells)[24] as well as the fraction of developing myeloid (Mac1$^+$Gr1$^+$) and erythroid (Ter119$^+$) cells were similar in *Prdm16*$^{-/-}$, *Prdm16*$^{+/-}$, and wt FL. T-cell development in the thymus (as measured by the fraction of lin$^-$CD25$^-$c-kit$^+$ early thymic precursors, CD4$^-$CD8$^-$ double-negative, CD4$^+$CD8$^+$ double-positive, and CD4 and CD8 single-positive cells)[25,26] of *Prdm16*$^{-/-}$, *Prdm16*$^{+/-}$, and wt embryos did not differ (not shown). Similarly, in adult *Prdm16*$^{+/-}$ mice, B, T, myeloid, and erythroid development was similar to that in wt mice (not shown).

Next, we phenotypically analyzed the stem and progenitor cell compartment of *Prdm16*-deficient mice. In *Prdm16*$^{-/-}$ E13.5 to 15.5 embryos, the frequency of LSK HSPCs, LSKCD150$^-$Flt3$^+$ MPPs, and in particular LSKCD150$^+$Flt3$^-$ HSCs[27] (FL HSCs, in contrast to adult HSCs, express CD34),[28,29] was decreased compared with wt littermates (Figure 2C-D). In *Prdm16*$^{+/-}$ FL, only the LSKCD150$^+$Flt3$^-$ fraction was decreased significantly (not shown). Similarly, adult *Prdm16*$^{+/-}$ mice showed reduced frequency of LT- and ST-HSCs, whereas MPPs were less profoundly affected (Figure 2E). As BM and FL cellularity were similar in wt and *Prdm16*-deficient mice (Figure 2A), these differences in HSPC frequencies are reflective of differences in absolute number.

These phenotypic data indicate that, consistent with predominant expression of *Prdm16* in the most primitive HSPC compartments, deletion of *Prdm16* decreases their frequency in BM and FL. *Prdm16* is furthermore haploinsufficient in this respect.

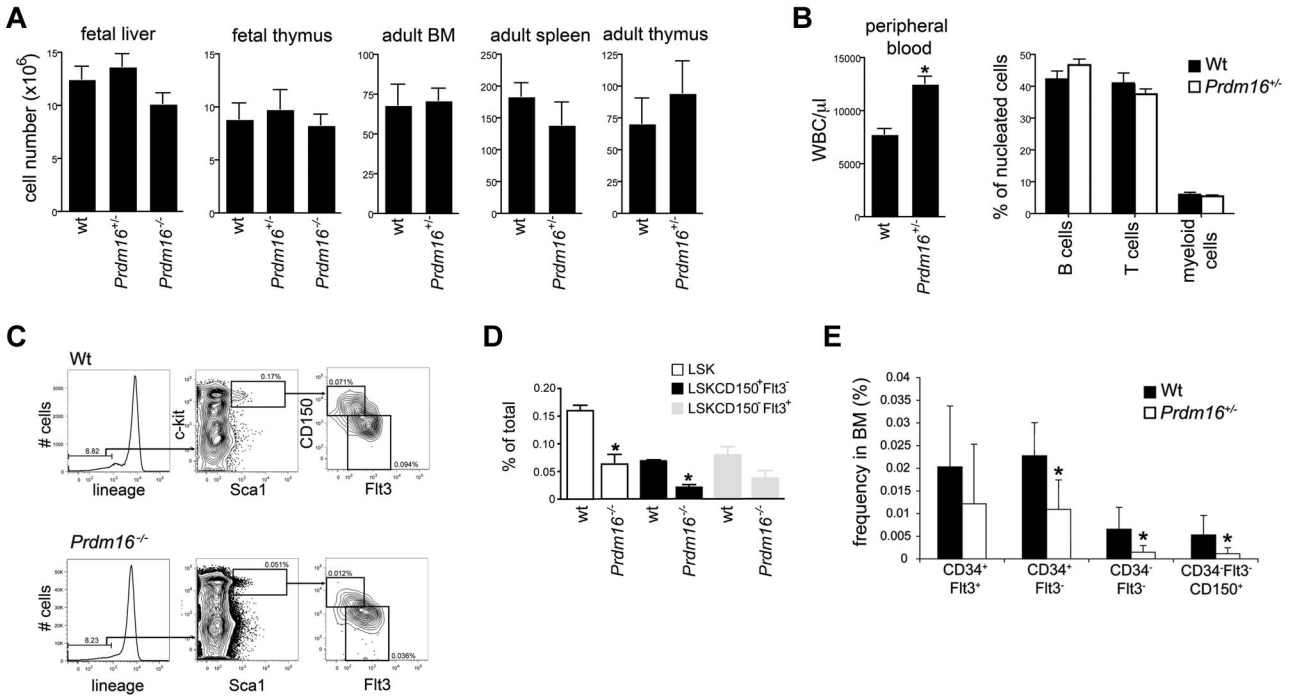


**Figure 2. Hematologic profile of *Prdm16*-deficient mice.** (A) Cellularity of FL and thymus, and of adult BM, thymus, and spleen in *Prdm16*-deficient mice (n = 3–5). (B) WBC count (left panel) and lineage distribution (measured by flow cytometric analysis of CD19, Thy1, and Mac1/Gr1) in the PB of adult $Prdm16^{+/-}$ and wt mice (n = 5). *$P = .0006$. (C) Representative example of flow cytometric analysis of the fraction of LSK HSPCs, LSK $CD150^{-}Flt3^{+}$ MPPs, and LSK $CD150^{+}Flt3^{-}$ HSCs in E15 $Prdm16^{-/-}$ and wt FL cells. (D) Frequency of the populations in panel C in E13.5 to E15.5 FL from $Prdm16^{-/-}$ and wt embryos. Frequencies obtained as the percentage of cells in doublet discriminated scatter (n = 4-6). *$P < .05$, one-way analysis of variance. (E) Frequencies of subpopulations of LSK cells in the BM of $Prdm16^{+/-}$ mice or wt littermates. Lineage cocktail included anti–CD41 and CD48 (n = 8). *$P < .03$.

### *Prdm16* deficiency causes a defect in HSCs

To assess progenitor function, we performed colony assays. Myeloid and erythroid colony formation was mildly affected compared with wt in $Prdm16^{+/-}$ (82% ± 3.5%, $P < .0001$) and $Prdm16^{-/-}$ (77% ± 3.5%, $P = .0003$) FL cells and adult BM cells (52% ± 4.1%, $P < .0001$) (n = 4 triplicate experiments for each genotype, not shown), indicating a subtle defect at the level of progenitor cells consistent with a limited decrease in phenotypically defined progenitors, such as MPPs. To assess HSC function, we performed competitive repopulation studies. We injected $0.5 \times 10^6$ wt littermate, $Prdm16^{+/-}$, or $Prdm16^{-/-}$ FL cells ($CD45.2^{+}$, B6.129 background) together with an equal number of T cell-depleted wt $CD45.1^{+}$ or $CD45.1^{+}CD45.2^{+}$ B6 BM cells into lethally irradiated B6.129F1 ($CD45.2^{+}$) hosts. T-cell depletion of competitors was performed to avoid both graft-versus-host disease and rejection of donor cells by competitor cells. T-cell reconstitution was not analyzed, as donor and recipient could not be distinguished, and as remaining host-derived hematopoietic cells are mostly T cells after lethal irradiation.[20] Although immunophenotypically defined HSCs were decreased 3-fold in $Prdm16^{-/-}$ FL, the contribution from $Prdm16^{-/-}$ cells to the myeloid and B lineages was 10-fold lower compared with that of wt FL and $Prdm16^{+/-}$ cells after 12 weeks (Figure 3A), and was undetectable after 5 months (Figure 3B). The contribution of $Prdm16^{+/-}$ FL cells was similar to that of wt cells after 12 weeks but was also severely reduced after 5 months (Figure 3A-B). Furthermore, in the BM, contribution of $Prdm16^{+/-}$ and in particular of $Prdm16^{-/-}$ FL cells to the LT-HSC, ST-HSC, and MPP compartments was extremely low compared with wt cells 5 months after transplantation, indicative of a severe defect in self-renewal capacity (Figure 3C). In competitive repopulation studies using adult BM, $Prdm16^{+/-}$ cells showed an initial repopulation defect in the myeloid lineage at 12 weeks (Figure 3D), probably a reflection of the fact that, because of their faster turnover, myeloid cells are a more sensitive indicator of HSC function. In the recipient BM, $Prdm16^{+/-}$ HSC contribution to all BM HSPC subfractions was decreased, however (Figure 3E). After transfer into secondary recipients, $Prdm16^{+/-}$ BM cells lost repopulation capacity compared with wt cells in the B lineage ($P = .02$, Figure 3F), whereas the loss in the myeloid lineage was near statistical significance ($P = .07$, Figure 3G).

To assure that the $CD45.2^{+}$ B and myeloid cells in the reconstituted recipients were from donor and not of host origin, we isolated $CD45.1^{+}CD45.2^{+}$ and $CD45.2^{+}$ cells that expressed either Mac1 (myeloid cells) or CD19 (B cells) from spleen of recipients of $Prdm16^{-/-}$ FL cells, extracted the genomic DNA, and amplified using primers specific for the wt or mutant *Prdm16* allele. In the $CD45.1^{+}CD45.2^{+}$ competitor cells, only the wt allele was detected, whereas in the $CD45.2^{+}$ donor population, only the mutant allele was observed (Figure 3H). These data confirm that the host did not contribute to the $CD45.2^{+}$ B and myeloid populations.

To confirm that the defect in competitive repopulation capacity was intrinsic to the HSCs, 300 FL LSK cells (Figure 4A), 500 adult BM LSK cells (Figure 4B), or 300 adult BM LT-HSCs ($LSKCD34^{-}Flt3^{-}$, Figure 4C) were transplanted together with $2 \times 10^5$ T cell–depleted $CD45.1^{+}$ or $CD45.1^{+}CD45.2^{+}$ B6 competitor cells into lethally irradiated B6.129F1 ($CD45.2^{+}$) mice. A representative example of the flow cytometric analysis of recipients of adult $Prdm16^{+/-}$ and wt LT-HSCs is shown in Figure 4B. For all cell populations tested, a defect in competitive repopulation of *Prdm16*-deficient cells was observed 12 to 16 weeks after transplantation. In recipients of adult BM LT-HSCs, we also analyzed contribution to developing T cells in the thymus ($CD4^{-}CD8^{-}$ double-negative and $CD4^{+}CD8^{+}$ double-positive cells), as in contrast to mature T cells, which are long-lived and relatively radioresistant, these cell populations turn over rapidly and can therefore not be derived from the host.

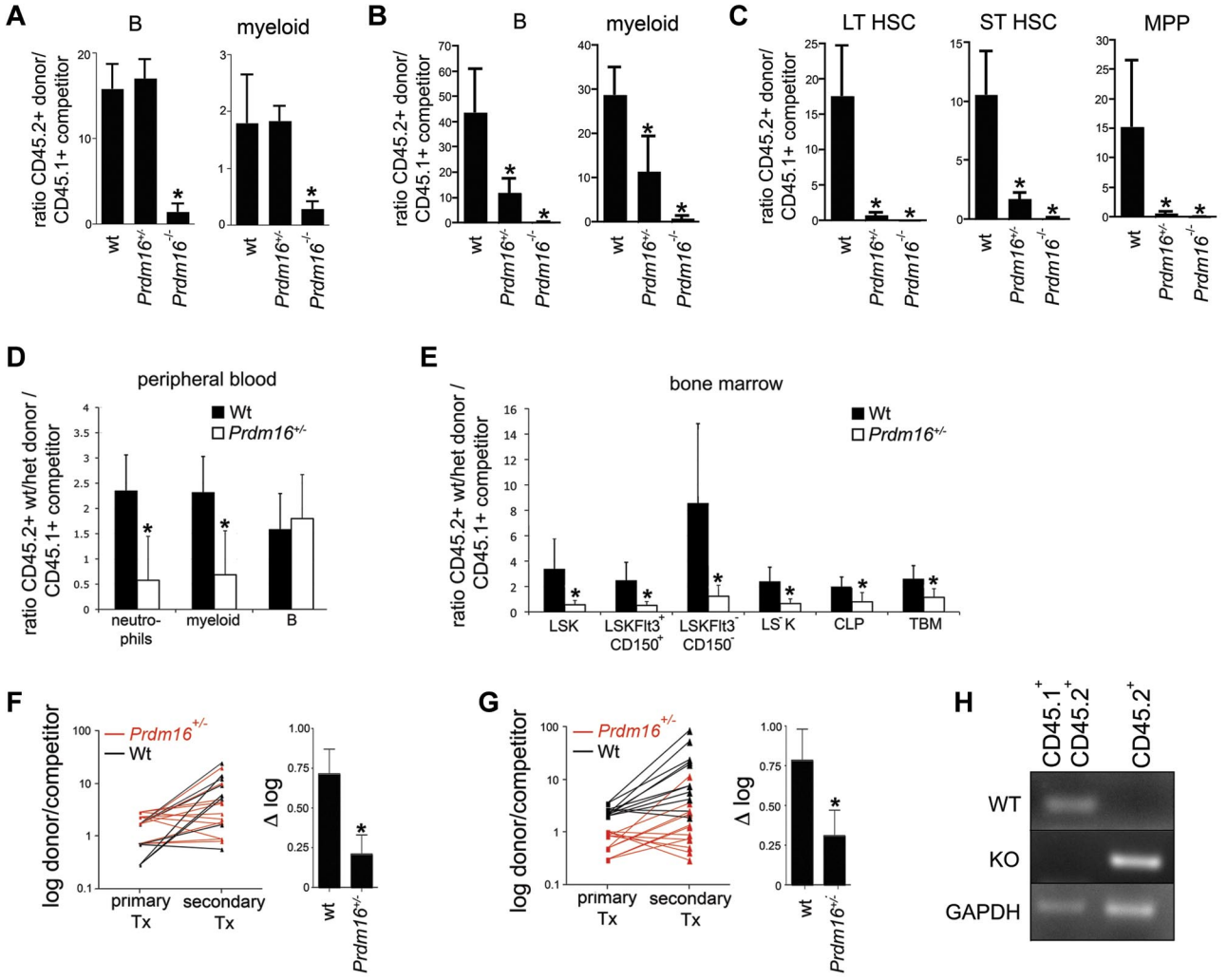


**Figure 3. Function of *Prdm16*–deficient FL and BM cells.** (A) Ratio between donor (*Prdm16*$^{-/-}$, *Prdm16*$^{+/-}$, or wt FL cells) and competitor (T cell–depleted CD45.1$^{+}$ or CD45.1$^{+}$CD45.2$^{+}$ B6 BM cells) cells among PB myeloid and B cells 12 weeks after transplantation of 0.5 × 10$^{6}$ cells of each population into lethally irradiated B6.129F1 (CD45.2$^{+}$) mice (n = 3 for wt, n = 12 for *Prdm16*$^{+/-}$, n = 14 for *Prdm16*$^{-/-}$). *$P$ < .01, one-way analysis of variance. (B-C) Ratio between donor (*Prdm16*$^{-/-}$, *Prdm16*$^{+/-}$, or wt FL cells) and competitor (T cell–depleted CD45.1$^{+}$ B6 BM cells) cells among PB myeloid and B cells (B) and among BM LT-HSCs, ST-HSCs, and MPPs (C) 20 weeks after transplantation as in panel A. (D-E) Competitive repopulation of 2 × 10$^{6}$ wt or *Prdm16*$^{+/-}$ BM cells (CD45.2$^{+}$) with 2 × 10$^{6}$ C57BL/6 (CD45.1$^{+}$) BM cells in B6.129F1 recipients after 12 to 16 weeks. Data presented as donor/competitor ratio within a specific compartment in PB (D) and BM (E) (n = 6). *$P$ < .02. TBM indicates total BM. (F-G) Shift in donor/competitor ratio within B cells (F) and myeloid cells (G) after serial transplantation of 2 × 10$^{6}$ BM cells from primary recipients into lethally irradiated secondary B6.129F1 CD45.2$^{+}$ recipients 12 to 14 weeks after primary transplantation. The right hand panels of panels F and G show the difference in log(donor/competitor) between primary and secondary recipients (n = 12 secondary recipients for each genotype). *$P$ = .07 for myeloid cells. *$P$ = .01 for B cells. Tx indicates transplantation. (H) Genomic PCR for the wt and mutant alleles in the myeloid and B cells of the spleens of recipients of CD45.2$^{+}$ *Prdm16*$^{-/-}$ cells and CD45.1$^{+}$CD45.2$^{+}$ B6 competitor cells.

The T-cell potential of *Prdm16*$^{+/-}$ cells was decreased to the same extent as their B and myeloid potential (Figure 4C-D).

We conclude that *Prdm16* is critical for HSC function, maintenance, and renewal and that this effect is intrinsic to HSCs and not dependent on the microenvironment.

### Enhanced apoptosis in *Prdm16*$^{-/-}$ HSCs

Next, we attempted to define a mechanism underlying the loss of HSCs in *Prdm16*-deficient mice. Homing of *Prdm16*$^{-/-}$, *Prdm16*$^{+/-}$, and wt FL cells was measured by injecting CFSE-labeled cells in lethally irradiated hosts, and determining the absolute number of CFSE-labeled cells that homed to the BM 3 hours after injection.[22] No difference in homing was observed (Figure 5A). These data argue against a homing defect in *Prdm16*-deficient HSPCs. Next, we analyzed cell cycle activity in FL HSPCs by staining using 4,6-diamidino-2-phenylindole. As cycling activity of HSPCs decreased with advancing fetal development (Figure 5B), data were normalized to those obtained from wt littermates (Figure 5C). Although a limited increase in cycling activity was observed in both *Prdm16*$^{+/-}$ and *Prdm16*$^{-/-}$ LSKFlt3$^{+}$ MPPs, this increase was just short of statistical significance in LSKFlt3$^{-}$ HSCs. Next, we examined apoptosis by staining fetal liver cells for annexin V. Compared with wt HSCs, the annexin V$^{+}$ fraction was increased in *Prdm16*$^{-/-}$ HSCs, but not in *Prdm16*$^{+/-}$ HSCs (Figure 5D). No difference in apoptosis was observed in MPPs (not shown) or in total FL cells (Figure 5D).

Thus, whereas cycling activity was mildly increased in the HSPC compartment, apoptosis was specifically increased in *Prdm16*$^{-/-}$ HSCs.

### Expression analysis of *Prdm16*$^{-/-}$ and wt HSCs

We used a microfluidic quantitative PCR array (Fluidigm)[30] to compare expression of a select set of genes in purified wt and

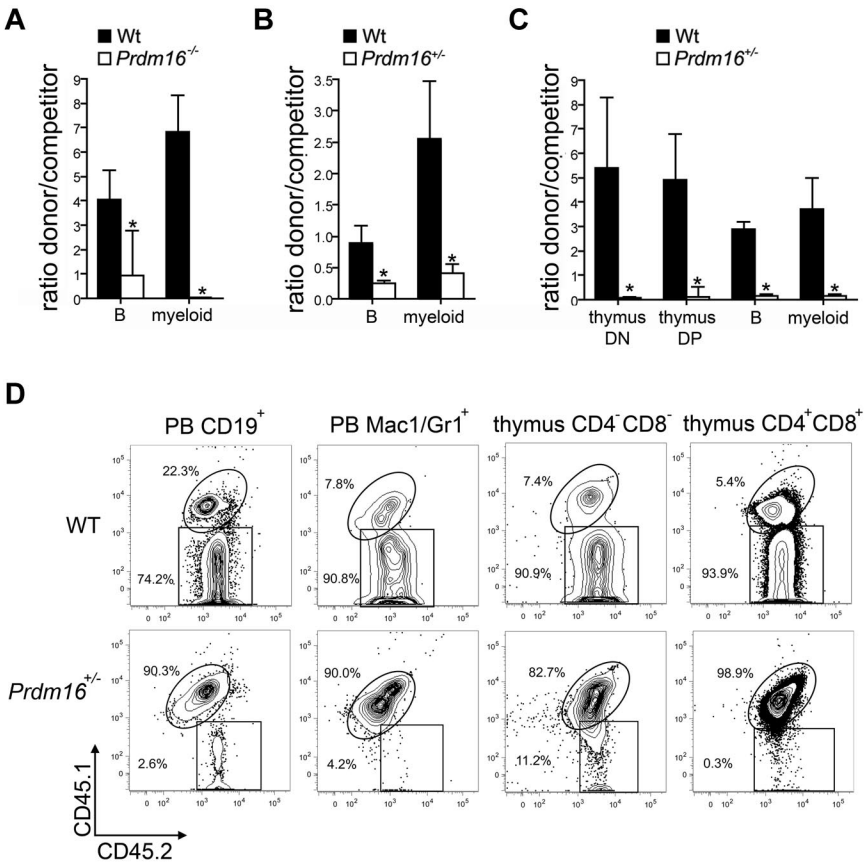


**Figure 4. Function of *Prdm16*-deficient HSPCs.** (A-C) Ratio between donor (300 *Prdm16*$^{-/-}$ or wt FL LSK cells (n = 4) (A), 500 *Prdm16*$^{+/-}$ or wt adult BM LSK cells (n = 9) (B), or 300 *Prdm6*$^{+/-}$ or wt adult BM LSKCD34$^{-}$Flt3$^{-}$ cells (n = 4) (C) and competitor ($0.5 \times 10^6$ T cell-depleted CD45.1$^{+}$ or CD45.1$^{+}$CD45.2$^{+}$ B6 BM cells) cells among PB myeloid and B cells, and (C) thymic CD4$^{+}$CD8$^{+}$ double-positive and CD4$^{-}$CD8$^{-}$ double-negative developing T cells, 10 to 15 weeks after transplantation into lethally irradiated B6.129F1 (CD45.2$^{+}$) mice. *$P < .01$. (D) Representative example of donor (CD45.2$^{+}$) and competitor (CD45.1$^{+}$CD45.2$^{+}$) reconstitution in doublet discriminated PB CD19$^{+}$ B and Mac1$^{+}$Gr1$^{+}$ myeloid cells, and in thymic CD4$^{-}$CD8$^{-}$ double-negative and CD4$^{+}$CD8$^{+}$ double-positive cells after competitive transplantation with wt or *Prdm16*$^{+/-}$ adult BM LT-HSCs.

*Prdm16*$^{-/-}$ FL HSCs. Five LSKCD150$^{+}$ FL cells were sorted per well. Eight triplicate groups of 5 *Prdm16*$^{-/-}$ and wt littermate HSCs were analyzed for the expression of 29 genes (Figure 6). Genes known to be involved in HSC function, renewal, and maintenance (*Bmi1, Pbx1, Evi1,* and *Gata2*),[5,31-33] apoptosis (*Trp53, Puma,* and *Tmbim4*),[34-38] cell cycle regulation (*Cdk4, Cdkn1a, Cdk1nb,* and *Ckdn1c*),[39,40] as well as cytokines and genes involved in cytokine signaling (*Notch1, Angpt1, Angpt2, Ryk, Wnt3a,* and *Smad2*)[41-45] were selected. *Prdm16*$^{-/-}$ neural stem cells (NSCs) have been reported to display increased oxidative stress.[46] Therefore, several genes previously reported to be decreased in *Prdm16*$^{-/-}$ ventricular zone NSCs (*Hgf, Lhcgr, Mt2, Pdk4, Crym, Ogn, Pparss2*, and *Hmgcs2*)[46] as well as 2 genes involved in oxidative stress and reported to be up-regulated in *Bmi1*$^{-/-}$ BM cells (*Alox5* and *Alox15*)[47] were examined. Finally, as Prdm16 interacts with the ligand-activated transcription factor peroxisome proliferator-activated receptor-γ and increases its ligand-induced transcriptional activity[18] in brown fat adipogenesis, we also measured expression of *Pparg* and its homolog, *Ppard*. Results are summarized in Figure 6.

No detectable signal was obtained for *Pdk4, Crym, Ogn, Pparss2*, and *Hmgcs2* (not shown). Other oxidative stress-responsive genes were expressed at similar levels in wt and *Prdm16*$^{-/-}$ HSCs, except for *Mt2*, expression of which was increased in *Prdm16*$^{-/-}$ HSCs and *Lhcgr*, which was lower (Figure 6). These data indicate that the mechanisms underlying the defects in HSC maintenance in *Prdm16*$^{-/-}$ mice probably differ from those involved in the reported defects in NSC function.[46]

The expression of the negative cell cycle regulators *Cdkn1a* and *Cdk1nb* was mildly higher in *Prdm16*$^{-/-}$ than in wt HSCs.

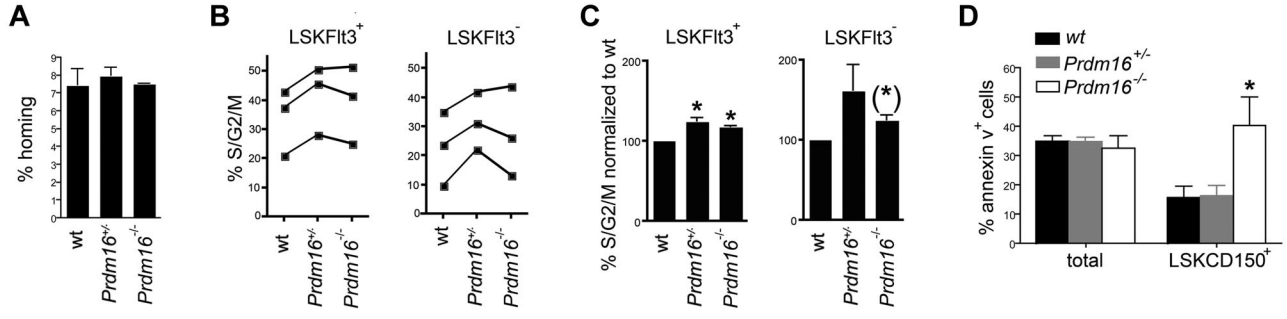


**Figure 5. Effects of Prdm16 on homing, apoptosis, and cell cycling.** (A) Homing of *Prdm16*$^{-/-}$, *Prdm16*$^{+/-}$, and wt E16 FL cells after transplantation into lethally irradiated CD45.1$^{+}$ recipients (n = 3). (B) Percentage of FL LSKFlt3$^{+}$ and LSKFlt3$^{-}$ cells from *Prdm16*$^{-/-}$, *Prdm16*$^{+/-}$, and wt mice in S/$G_2$/M phase of the cell cycle as measured by 4,6-diamidino-2-phenylindole staining. Each experiment contained 2 to 4 embryos per genotype. (C) Fraction of FL LSKFlt3$^{+}$ and LSKFlt3$^{-}$ cells from *Prdm16*$^{-/-}$, *Prdm16*$^{+/-}$, and wt mice in S/$G_2$/M phase normalized to the values of wt littermate embryos (n = 3 litters). *$P < .05$. (*)$P = .08$. (D) Percentage of apoptotic total FL and LSKCD150$^{+}$ FL cells in *Prdm16*$^{-/-}$, *Prdm16*$^{+/-}$, and wt embryos (n = 3 for each genotype). *$P = .05$, one-way ANOVA.

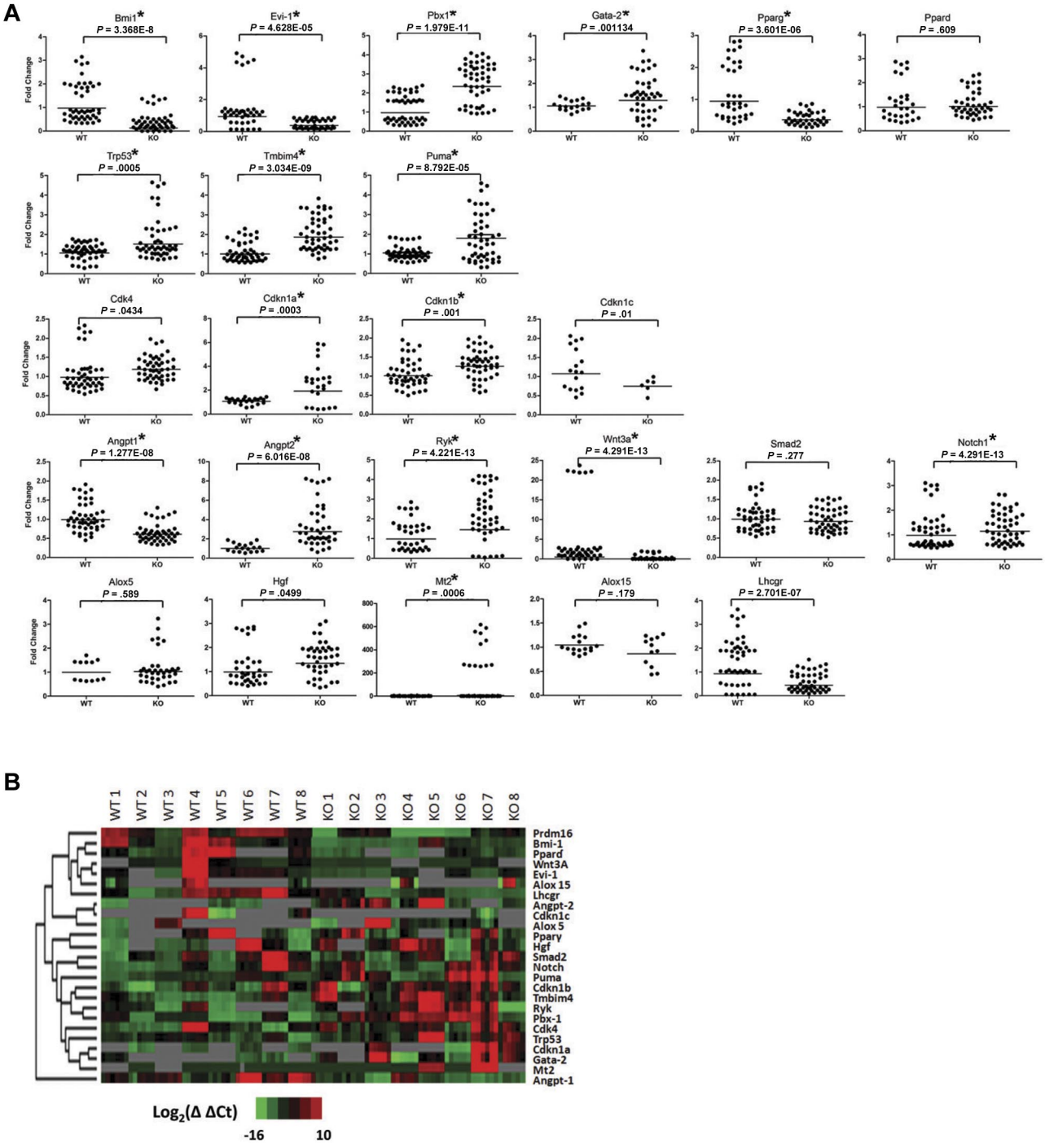


**Figure 6. Expression analysis of *Prdm16*$^{-/-}$ and wt FL HSCs.** (A) Scatter dot plots of the expression of the genes, as measured using Fluidigm multiplex quantitative PCR, indicated on top of each panel in 8 groups of 5 *Prdm16*$^{-/-}$ or wt FL LSKCD150$^{+}$ HSCs. *$P < .002$, threshold required after Bonferroni correction. All experimental replicates of the amplification step and the microfluidic quantitative PCR chip are shown. Undetectable expression is defined by a $C_t$ value of 35 or greater. (B) Heat map of the expression levels for *Prdm16* and 24 genes shown in panel A.

Expression of *Trp53* (*p53*) and one of its prime transcriptional targets, *Puma*,[34] as well as that of the potential Bax inhibitor *Tmbim4* was higher in *Prdm16*$^{-/-}$ than in wt HSCs. These observations may explain the increased apoptosis observed in *Prdm16*$^{-/-}$ HSCs. Several transcriptional regulators that are known to be critical for HSC maintenance[5,31-33] were differentially expressed in wt and *Prdm16*$^{-/-}$ HSCs. Expression of *Bmi1* and *Evi1* was lower, whereas expression of *Pbx1* and *Gata2* was higher in *Prdm16*$^{-/-}$ than in wt HSCs. A profound decrease in *Pparg* expression was observed in *Prdm16*$^{-/-}$ HSCs. Expression of the *Ppar* family member *Ppard* was similar in wt and *Prdm16*$^{-/-}$ HSCs, however. Finally, the expression of the number of cytokines and cytokine receptors was significantly different in wt and *Prdm16*$^{-/-}$ cells. Expression of *Angpt1* and *Wnt3a* was suppressed, whereas expression of the Wnt receptor *Ryk*[48] (which has been reported to be expressed specifically in LT-HSCs)[45] and of *Angpt2* was increased. Taken together, these data suggest that *Prdm16* regulates HSCs through multiple, and sometimes opposing, mechanisms.

## Discussion

We have shown here that, within the hematopoietic system, *Prdm16* is expressed very selectively in the earliest stem and progenitor compartments, and, consistent with this expression pattern, is required for the maintenance of the HSC pool during development and after transplantation.

A HSC defect in *Prdm16*$^{-/-}$ mice was also very recently described by Chuikov et al.[46] We noted some differences in our studies. Although many of their experiments were performed using cells isolated from newborn mice, we never observed live-born *Prdm16*$^{-/-}$ pups. As the origin of the mice used in our studies was the same as that of the mice used in the studies of Chuikov et al,[46] the cause of this difference is unclear but may be related to the backcrossing of *Prdm16*$^{-/-}$ mice onto C57Bl/6 background in their study. We also observed leukocytosis in adult *Prdm16*$^{+/-}$ mice. Given the normal cellularity of hematopoietic organs and the profound HSC defect observed after transplantation of *Prdm16*$^{+/-}$ BM or purified HSPCs, this finding is probably explained by an organismal effect of *Prdm16* that is independent of its cell autonomous role in HSCs. Furthermore, Chuikov et al[46] did not observe a defect in HSC number and function in heterozygous *Prdm16*$^{+/-}$ mice, although they did report an NSC defect in *Prdm16*$^{+/-}$ mice. In contrast, we found that *Prdm16* displays both expression and functional haploinsufficiency with respect to HSC function. This difference, too, may be the result of the different genetic background of the mice used in our studies (B6.126) compared with the studies of Chuikov et al,[46] where the mice were backcrossed onto the C57BL/6 background. Haploinsufficiency has previously been described in *Evi1*-deleted mice.[5] The phenotype of *Evi1*$^{-/-}$ mice is qualitatively remarkably similar, although quantitatively more severe, compared with that of *Prdm16*$^{-/-}$ mice.[5] As *Evi1* expression was down-regulated in *Prdm16*$^{-/-}$ HSCs (Figure 6), *Prdm16* may act, at least in part, through regulation of *Evi1* expression.

The mechanism of action of Prdm16 is probably more complex, however. Maintenance of the HSC function in the long-term requires a critical balance between renewing and differentiating proliferation, quiescence, and survival, as well as appropriate homeostatic responses to damage and stress.[1,34] Both in mouse models where HSC quiescence is increased, such as *Mef*$^{-/-}$ and *Bmi1*$^{-/-}$ mice,[31,49] and in models where HSC cell cycle activity is increased, such as *Gfi*$^{-/-}$, *Evi1*$^{-/-}$, and *Pbx1*$^{-/-}$ mice,[5,33,50] long-term HSC function is severely compromised. *Prdm16*$^{-/-}$ NSCs have been reported to display increased oxidative stress and to express less hepatocyte growth factor (*Hgf*) mRNA. Addition of HGF could partially reverse the NSC defect in *Prdm16*$^{-/-}$ mice.[46] We examined the expression of genes, including *Hgf*, which were down-regulated in *Prdm16*$^{-/-}$ NSCs.[46] Only one of those, luteinizing hormone/choriogonadotropin receptor (*Lhcgr*) was also decreased in *Prdm16*$^{-/-}$ HSCs, whereas another gene, *Mt2* (metallothionein 2), a reported indirect target of Prdm16,[46] was actually increased in HSCs, rather than decreased, as was reported for NSCs.[46] Furthermore, the expression of 2 genes involved in oxidative stress responses and up-regulated in the BM of *Bmi1*$^{-/-}$ mice, *Alox5* and *Alox15*, was also similar in *Prdm16*$^{-/-}$ and wt HSCs.[47] These observations suggest that the mechanisms underlying the HSC defect in *Prdm16*-deficient mice may be partially overlapping with, but are nevertheless substantially different from, those causing the NSC defect.

At least one of the mechanisms underlying the HSC defect in *Prdm16*$^{-/-}$ mice may be increased apoptosis. Consistent with this finding, expression of *Trp53* (p53) and its prime target, *Puma*,[34] as well as *Tmbim4*, a potential Bax inhibitor,[38] was increased. *Trp53*$^{-/-}$ mice have an expanded HSPC compartment,[34,35] whereas *Puma*$^{-/-}$ mice are resistant to hematopoietic failure caused by irradiation and cytotoxic drugs.[36,37] It is interesting to note, however, that *Prdm16* deletion affects transcription or stability of p53 mRNA, as *p53* is typically regulated post-transcriptionally.[34] An interesting observation made by Chuikov et al is that, in contrast to NSCs, *Prdm16*$^{-/-}$ HSCs appeared to contain lower levels of reactive oxygen species than wt HSCs.[46] This is surprising as we found decreased *Bmi1* expression in *Prdm16*$^{-/-}$ HSCs and as *Bmi1* deletion causes increased oxidative stress.[47] As p53 has been shown to decrease oxidative stress in some conditions,[51] it is possible that this observation is, at least in part, explained by increased *p53* expression in *Prdm16*$^{-/-}$ HSCs. Somewhat puzzling was that no significant increase in the fraction of apoptotic cells was observed in *Prdm16*$^{+/-}$ HSCs. It is possible that the difference between wt and *Prdm16*$^{+/-}$ HSCs with respect to apoptosis as determined by annexin V staining was too subtle to detect. However, given the severity of the HSC defect in *Prdm16*$^{+/-}$ mice, which quantitatively approached that of *Prdm16*$^{-/-}$ mice, it is more likely that *Prdm16* affects HSC function through multiple mechanisms and that the threshold level of *Prdm16* expression required to affect these mechanisms varies.

This possibility is strongly suggested by the subtle but consistent increase in cell cycle activity in the HSPC compartment that was, in contrast to the fraction of apoptotic cells, similar in *Prdm16*$^{+/-}$ and *Prdm16*$^{-/-}$ mice. It is unclear whether this increase in cycling activity is a result of selective depletion of quiescent HSCs, or of more generally enhanced cycling activity of the HSC compartment, or both. Interestingly, expression analysis revealed increased expression of several genes that are negative regulators of cell cycling in HSPCs.[34,35,39,40] These include, in addition to p53, *Cdkn1a* (p21) and *Cdkn1b* (p27). Furthermore, one of the most striking results of our expression analysis was decreased *Bmi1* expression in *Prdm16*$^{-/-}$ HSCs. *Bmi1* is a polycomb gene that suppresses the expression of the tumor suppressors *p16*$^{ink4a}$ and *p19*$^{arf}$ and is critical for HSC renewal.[31,52] Prdm16 must therefore affect cell cycling through multiple opposing mechanisms.

Prdm16 directly or indirectly regulates a remarkable number of transcriptional regulators that are critical for HSC function and act through overlapping but probably distinct mechanisms. Some of the genes that are critical for HSC function, such as *Evi1* and *Bmi1*, are down-regulated,[5,31] but others, such as *Gata2* and *Pbx1*,[32,33] are up-regulated. Furthermore, *p53*, a negative regulator of HSC function,[34,35] is up-regulated. Thus, Prdm16 induces changes in HSCs that, based on well-characterized knockout models, both enhance and suppress HSC function, and affect quiescence, cell cycling, renewal, differentiation, and apoptosis to various extents. These expression data suggest that Prdm16 may be a critical node in a network that contains negative and positive feedback loops and regulates and integrates HSC renewal, quiescence, differentiation, and apoptosis. The role of PPAR family members in HSCs is unclear. *Pparg* and *Ppard*, but not *Ppara*, are expressed in HSCs (not shown). *Prdm16* deletion decreases expression of *Pparg* mRNA. The transcriptional activity of Pparg is enhanced by Prdm16 during brown fat adipogenesis.[18] The fact that *Prdm16* deletion decreases expression of a transcription factor of which it increases the activity suggests a positive feedback loop. It will therefore be of interest to examine the effect of deletion of *Pparg*

and to study any compensatory effects of both *Pparg* and *Ppard* on HSC function.

Our expression data also suggest a role for *Prdm16* in the regulation of autocrine and paracrine signaling in and among HSCs and suggest that cell autonomously produced cytokines and their receptors may be part of this HSC regulatory network. Expression of *Angpt1* (Angiopoietin-1 or Ang-1) was suppressed in *Prdm16*$^{-/-}$ HSCs. Ang-1 enhances HSC quiescence by signaling through Tie-2.[41] On the other hand, expression of *Angpt2* (Ang-2), which antagonizes Ang-1-induced Tie-2 signaling,[42] was increased. Furthermore, the decrease of *Wnt3a* expression in *Prdm16*$^{-/-}$ HSCs is of interest and may explain part of the HSC defect. FL *Wnt3a*$^{-/-}$ HSCs show a repopulation defect after transplantation into adult recipients.[43] Whereas one interpretation of these findings is that HSCs generated in a Wnt3a-deficient environment are functionally abnormal, another, possibly more plausible explanation may be that cell autonomous production of Wnt3a is critical for sustained HSC function. It is also interesting to note that *Ryk*, a noncanonical Wnt receptor that has been shown to be relatively specifically expressed in LT-HSCs,[45,48] is also regulated directly or indirectly by *Prdm16*.

Taken together, we have shown here that *Prdm16* plays a critical role in long-term HSC maintenance and renewal. *Prdm16* is probably a major and integrative node in a network that involves at the very least *Evi1*, *Pbx1*, *Gata2*, *Bmi1*, the downstream *Bmi1* targets *p16*$^{inka}$ and *p19*$^{arf}$, *p53* and its targets, as well as cytokine receptors and cell autonomously produced cytokines, and regulates HSC renewal, cycling, and apoptosis.

## Acknowledgments

This work was supported by the National Institutes of Health (grants RO1 HL073760 and RO1 AG 016327; H.-W.S.).

## Authorship

Contribution: F.A. performed hematopoietic profile analysis, studies using purified progenitor and stem cells, expression studies, homing, and apoptosis; S.A. performed studies in adult mice; A.L. and P.K. assisted in most experiments; A.S., D.-F.L., and I.R.L. assisted and provided advice in microfluidics array expression analysis; B.Y.Z. performed part of the studies on fetal mice; and H.-W.S. designed experiments, analyzed the data, and wrote the manuscript.

Conflict-of-interest disclosure: The authors declare no competing financial interests.

Correspondence: Hans-Willem Snoeck, Department of Gene and Cell Medicine, Mount Sinai of School of Medicine, Gustave L. Levy Place, Box 1496 New York, NY 10029; e-mail: hans.snoeck@mssm.edu.

## References

1. Orkin SH, Zon LI. Hematopoiesis: an evolving paradigm for stem cell biology. *Cell.* 2008;132(4):631-644.
2. Ernst P, Fisher JK, Avery W, et al. Definitive hematopoiesis requires the mixed-lineage leukemia gene. *Dev Cell.* 2004;6(3):437-443.
3. McMahon KA, Hiew SY, Hadjur S, et al. Mll has a critical role in fetal and adult hematopoietic stem cell self-renewal. *Cell Stem Cell.* 2007;1(3):338-345.
4. Jude CD, Climer L, Xu D, Artinger E, Fisher JK, Ernst P. Unique and independent roles for MLL in adult hematopoietic stem cells and progenitors. *Cell Stem Cell.* 2007;1(3):324-337.
5. Goyama S, Yamamoto G, Shimabe M, et al. Evi-1 is a critical regulator for hematopoietic stem cells and transformed leukemic cells. *Cell Stem Cell.* 2008;3(2):207-220.
6. Okuda T, van Deursen J, Hiebert SW, Grosveld G, Downing JR. AML1, the target of multiple chromosomal translocations in human leukemia, is essential for normal fetal liver hematopoiesis. *Cell.* 1996;84(2):321-330.
7. Wang Q, Stacy T, Binder M, Marin-Padilla M, Sharpe AH, Speck NA. Disruption of the Cbfa2 gene causes necrosis and hemorrhaging in the central nervous system and blocks definitive hematopoiesis. *Proc Natl Acad Sci U S A.* 1996;93(8):3444-3449.
8. Shivdasani RA, Mayer EL, Orkin SH. Absence of blood formation in mice lacking the T-cell leukaemia oncoprotein tal-1/SCL. *Nature.* 1995;373:432-434.
9. Robb L, Lyons I, Li R, et al. Absence of yolk sac hematopoiesis from mice with a targeted disruption of the scl gene. *Proc Natl Acad Sci U S A.* 1995;92(15):7075-7079.
10. Mochizuki N, Shimizu S, Nagasawa T, et al. A novel gene, MEL1, mapped to 1p36.3 is highly homologous to the MDS1/EVI1 gene and is transcriptionally activated in t(1;3)(p36;q21)-positive leukemia cells. *Blood.* 2000;96(9):3209-3214.
11. Nishikata I, Sasaki H, Iga M, et al. novel EVI1 gene family, MEL1, lacking a PR domain (MEL1S) is expressed mainly in t(1;3)(p36;q21)-positive AML and blocks G-CSF-induced myeloid differentiation. *Blood.* 2003;102(9):3323-3332.
12. Sakai I, Tamura T, Narumi H, et al. Novel RUNX1-PRDM16 fusion transcripts in a patient with acute myeloid leukemia showing t(1;21)(p36;q22). *Genes Chromosomes Cancer.* 2005;44(3):265-270.
13. Roche-Lestienne C, Deluche L, Corm S, et al. RUNX1 DNA-binding mutations and RUNX1-PRDM16 cryptic fusions in BCR-ABL+ leukemias are frequently associated with secondary trisomy 21 and may contribute to clonal evolution and imatinib resistance. *Blood.* 2008;111(7):3735-3741.
14. Shing DC, Trubia M, Marchesi F, et al. Overexpression of sPRDM16 coupled with loss of p53 induces myeloid leukemias in mice. *J Clin Invest.* 2007;117(12):3696-3707.
15. Du Y, Jenkins NA, Copeland NG. Insertional mutagenesis identifies genes that promote the immortalization of primary bone marrow progenitor cells. *Blood.* 2005;106(12):3932-3939.
16. Deneault E, Cellot S, Faubert A, et al. A functional screen to identify novel effectors of hematopoietic stem cell activity. *Cell.* 2009;137(2):369-379.
17. Kajimura S, Seale P, Kubota K, et al. Initiation of myoblast to brown fat switch by a PRDM16-C/EBP-beta transcriptional complex. *Nature.* 2009;460(7259):1154-1158.
18. Seale P, Bjork B, Yang W, et al. PRDM16 controls a brown fat/skeletal muscle switch. *Nature.* 2008;454(7207):961-967.
19. Zambrowicz BP, Abuin A, Ramirez-Solis R, et al. Wnk1 kinase deficiency lowers blood pressure in mice: a gene-trap screen to identify potential targets for therapeutic intervention. *Proc Natl Acad Sci U S A.* 2003;100(24):14109-14114.
20. Avagyan S, Amrani Y, Snoeck HW. Isolation and analysis of mouse hematopoietic stem cells. *Methods Enzymol.* 2010;476:429-447.
21. Langer JC, Henckaerts E, Orenstein J, Snoeck HW. Quantitative trait analysis reveals transforming growth factor-beta2 as a positive regulator of early hematopoietic progenitor and stem cell function. *J Exp Med.* 2004;199(1):5-14.
22. Foudi A, Jarrier P, Zhang Y, et al. Reduced retention of radioprotective hematopoietic cells within the bone marrow microenvironment in CXCR4−/− chimeric mice. *Blood.* 2006;107(6):2243-2251.
23. Challen GA, Boles N, Lin KK, Goodell MA. Mouse hematopoietic stem cell identification and analysis. *Cytometry A.* 2009;75(1):14-24.
24. Hardy RR, Kincade PW, Dorshkind K. The protean nature of cells in the B lymphocyte lineage. *Immunity.* 2007;26(6):703-714.
25. Godfrey DI, Kennedy J, Suda T, Zlotnik A. A developmental pathway involving four phenotypically and functionally distinct subsets of CD3-CD4-CD8- triple-negative adult mouse thymocytes defined by CD44 and CD25 expression. *J Immunol.* 1993;150(10):4244-4252.
26. Allman D, Sambandam A, Kim S, et al. Thymopoiesis independent of common lymphoid progenitors. *Nat Immunol.* 2003;4(2):168-174.
27. Kim I, He S, Yilmaz OH, Kiel MJ, Morrison SJ. Enhanced purification of fetal liver hematopoietic stem cells using SLAM family receptors. *Blood.* 2006;108(2):737-744.
28. Matsuoka S, Ebihara Y, Xu M, et al. CD34 expression on long-term repopulating hematopoietic stem cells changes during developmental stages. *Blood.* 2001;97(2):419-425.
29. Osawa M, Hanada K, Hamada H, Nakauchi H. Long-term lymphohematopoietic reconstitution by a single CD34-low/negative hematopoietic stem cell. *Science.* 1996;273(5272):242-245.
30. Frederickson RM. Fluidigm: biochips get indoor plumbing. *Chem Biol.* 2002;9(11):1161-1162.
31. Park IK, Qian D, Kiel M, et al. Bmi-1 is required for maintenance of adult self-renewing haematopoietic stem cells. *Nature.* 2003;423(6937):302-305.
32. Tsai FY, Keller G, Kuo FC, et al. An early haematopoietic defect in mice lacking the transcription factor GATA-2. *Nature.* 1994;371(6494):221-226.

33. Ficara F, Murphy MJ, Lin M, Cleary ML. Pbx1 regulates self-renewal of long-term hematopoietic stem cells by maintaining their quiescence. *Cell Stem Cell.* 2008;2(5):484-496.
34. Asai T, Liu Y, Bae N, Nimer SD. The p53 tumor suppressor protein regulates hematopoietic stem cell fate. [published online ahead of print December 6, 2010] *J Cell Physiol.* doi: 10.1002/jcp.22561.
35. Liu Y, Elf SE, Miyata Y, et al. p53 regulates hematopoietic stem cell quiescence. *Cell Stem Cell.* 2009;4(1):37-48.
36. Shao L, Sun Y, Zhang Z, et al. Deletion of proapoptotic Puma selectively protects hematopoietic stem and progenitor cells against high-dose radiation. *Blood.* 2010;115(23):4707-4714.
37. Yu H, Shen H, Yuan Y, et al. Deletion of Puma protects hematopoietic stem cells and confers long-term survival in response to high-dose gamma-irradiation. *Blood.* 2010;115(17):3472-3480.
38. Reimers K, Choi CY, Bucan V, Vogt PM. The Bax Inhibitor-1 (BI-1) family in apoptosis and tumorigenesis. *Curr Mol Med.* 2008;8(2):148-156.
39. Cheng T, Rodrigues N, Shen H, et al. Hematopoietic stem cell quiescence maintained by p21cip1/waf1. *Science.* 2000;287(5459):1804-1808.
40. Cheng T, Rodrigues N, Dombkowski D, Stier S, Scadden DT. Stem cell repopulation efficiency but not pool size is governed by p27(kip1). *Nat Med.* 2000;6(11):1235-1240.
41. Arai F, Hirao A, Ohmura M, et al. Tie2/angiopoietin-1 signaling regulates hematopoietic stem cell quiescence in the bone marrow niche. *Cell.* 2004;118(2):149-161.
42. Gomei Y, Nakamura Y, Yoshihara H, et al. Functional differences between two Tie2 ligands, angiopoietin-1 and -2, in regulation of adult bone marrow hematopoietic stem cells. *Exp Hematol.* 2010;38(2):82-89.
43. Luis TC, Weerkamp F, Naber BA, et al. Wnt3a deficiency irreversibly impairs hematopoietic stem cell self-renewal and leads to defects in progenitor cell differentiation. *Blood.* 2009;113(3):546-554.
44. Maillard I, Koch U, Dumortier A, et al. Canonical notch signaling is dispensable for the maintenance of adult hematopoietic stem cells. *Cell Stem Cell.* 2008;2(4):356-366.
45. Forsberg EC, Passegué E, Prohaska SS, et al. Molecular signatures of quiescent, mobilized and leukemia-initiating hematopoietic stem cells. *PLoS ONE.* 2010;5(1):e8785.
46. Chuikov S, Levi BP, Smith ML, Morrison SJ. Prdm16 promotes stem cell maintenance in multiple tissues, partly by regulating oxidative stress. *Nat Cell Biol.* 2010;12(10):999-1006.
47. Liu J, Cao L, Chen J, Song S, et al. Bmi1 regulates mitochondrial function and the DNA damage response pathway. *Nature.* 2009;459(7245):387-392.
48. Fradkin LG, Dura JM, Noordermeer JN. Ryks: new partners for Wnts in the developing and regenerating nervous system. *Trends Neurosci.* 2010;33(2):84-92.
49. Lacorazza HD, Yamada T, Liu Y, et al. The transcription factor MEF/ELF4 regulates the quiescence of primitive hematopoietic cells. *Cancer Cell.* 2006;9(3):175-187.
50. Hock H, Hamblen MJ, Rooke HM, et al. Gfi-1 restricts proliferation and preserves functional integrity of haematopoietic stem cells. *Nature.* 2004;431(7011):1002-1007.
51. Sablina AA, Budanov AV, Ilyinskaya GV, Agapova LS, Kravchenko JE, Chumakov PM. The antioxidant function of the p53 tumor suppressor. *Nat Med.* 2005;11(12):1306-1313.
52. Oguro H, Iwama A, Morita Y, Kamijo T, van Lohuizen M, Nakauchi H. Differential impact of Ink4a and Arf on hematopoietic stem cells and their bone marrow microenvironment in Bmi1-deficient mice. *J Exp Med.* 2006;203(10):2247-2253.